Energy calibration and data processing of the LXe/CsI-combined calorimeter of the CMD-3 detector

Aleksandr Semenov*, *Andrei* Grebenuk, *Alexey* Kozyrev, *Terentii* Kuznetsov, *Kirill* Mikhailov, *Vasily* Shebalin, and *Boris* Shwartz

Abstract. The physics program of the symmetric electron-positron collider VEPP-2000 includes high-precision measurements of the $e^+e^- \to hadrons$ cross-sections in the energy range from the production threshold to 2 GeV. These precise data are highly demanded for a calculation of the hadronic contribution to the muon anomalous magnetic moment $(g-2)_\mu$ in the frame of the Standard Model as well as for the verification of various theoretical models of light hadrons interactions. The CMD-3 detector under operation now at VEPP-2000 combines properties of the magnetic spectrometry with a high-resolution electromagnetic calorimeter. One of the key detector subsystem is a high quality electromagnetic calorimeter. The barrel calorimeter of this detector consists of an inner part with coaxially arranged liquid xenon (LXe) and an outer part based on CsI crystals. This combined structure of the calorimeter provides a high photon coordinate measurement as well as a good energy resolution. However, this combined structure requires special sophisticated procedures for the energy calibration and photon reconstruction which are discussed in this proceeding.

1 Introduction

The physics program of the symmetric electron-positron collider VEPP-2000 [1] includes high-precision measurements of the $e^+e^- > hadrons$ cross-sections in the energy range from the production threshold to 2 GeV. These precise data are highly demanded for a calculation of the hadronic contribution to the muon anomalous magnetic moment $(g-2)_\mu$ in the frame of the Standard Model as well as for the verification of various thoretical models of light hadrons interactions. The high collider luminosity (up to $1 \times 10^{32}\,\mathrm{cm}^{-2}\,\mathrm{s}^{-1}$) is provided by a special feature that involves using the circular beam cross section concept. The VEPP-2000 has two interactions regions occupied with CMD-3 [2] and SND [3] detectors.

The CMD-3 detector is the cryogenic magnetic detector. The structure of the detector is shown in Fig. 1. The CMD-3 magnetic spectrometry is provided by the cylindrical drift chamber (DC) located inside the superconducting solenoid that generates a magnetic field of 1.3 T. The combined barrel electromagnetic calorimeter is placed coaxially outside of the superconducting solenoid. This calorimeter includes the liquid xenon (LXe) in the inner part and CsI crystals in the outer part. The time of flight (TOF) system is installed in the gap between the LXe and CsI-calorimeters. The small angle area occupied by the endcap calorimeter based on the $Bi_4Ge_3O_{12}$ (BGO) crystals comprises the area near the beam pipe. A muon-system (Mu) from plastic scintillator counters covers the iron yoke.

The structure of the LXe-calorimeter [4] represents alternating 8 anode and 7 cathode cylindrical layers, which

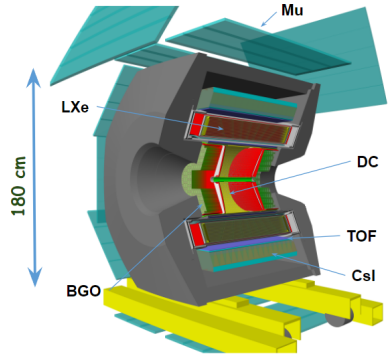

Figure 1: The design of the CMD-3 detector.

form 15 coaxial cylindrical ionization chambers. Anodes have a pad pattern. Each anode layer is divided into 264 cells (33 along the azimuth angle and 8 along the Z-axis). Cells with the common angle coordinate are electrically connected forming one tower of the calorimeter, which is used to measure particle energy. The cathode layers have orthogonal strips on the both sides to determine the particle coordinates layer by layer. The total thickness of the LXe-calorimeter is $5.4X_0$.

The CsI-calorimeter [5] consists of 1152 scintillation crystals compiled into 8 octants. The crystals (doped Tl and Na) have a rectangular shape with dimensions $6 \times 6 \times 15\,\mathrm{cm}^3$. The crystal length corresponds to $8.1X_0$. The combined structure of the cylindrical calorimeter provides precision measurements of photon positioning as well as a good energy resolution. The photon conversion point in the LXe calorimeter can be measured with the res-

*e-mail: Al.Vl.Semenov@inp.nsk.su

© The Authors, published by EDP Sciences. This is an open access article distributed under the terms of the Creative Commons Attribution License 4.0 (https://creativecommons.org/licenses/by/4.0/).

olution of about 2 mm. In addition, the charged particle track can be reconstructed using the LXe strip system, and the spatial distribution of its energy deposition measured by the strips can be used for particle identification. It is worth noting that the accurate photon coordinate measurements are significant for the reconstruction of the neutral pion invariant mass at high momenta. The total thickness of the barrel calorimeter is $13.5X_0$. However, this combined structure requires special sophisticated procedures for the energy calibration, photon reconstruction and quality monitoring.

2 Energy calibration

The energy deposited in the calorimeters is determined as:

$$E = k \cdot (A - p),$$

where A — ADC amplitude, p — ADC pedestal and k — conversion factor. The pedestal value is measured using a generator trigger while k-factor determination requires a special energy calibration procedure. Simultaneous energy calibration of LXe and CsI systems is performed using the background events with cosmic ray particles selected from the experimental data set. The example of such event is shown in the Fig. 2. Most of the cosmic ray particles crossing the calorimeters are minimum ionizing/ionising particles (MIPs).

The cosmic ray track is reconstructed in the LXe calorimeter and extrapolated to the CsI. Then we know the path length of the particle in the crossed crystals and LXe towers and calculate the value of dE/dx. The calibration constant k is obtained by comparing of the peak value of the dE/dx distribution for each crystal and LXe tower with the corresponding value of the dE/dx distribution obtained by the simulation. The simulation results in the following values: $\epsilon^{mc}_{CsI,LXe} = 0.604\,\mathrm{MeV/mm}$ and $0.3725\,\mathrm{MeV/mm}$. Finally, the value $dE/dx = E/d$ is obtained for each channel. As a result of each calibration run the corrections to the previous conversion factor set is determined which is equal to $\varepsilon^{mc}/\varepsilon^{exp}$. The result of this energy calibration is consistent with the 1% accuracy with the simulation for MIPs from beams collisions (see Fig. 7) and with the 2% accuracy for electrons and positrons (see Fig. 8). The inconsistency in the electron-positron datasets before 2014 is induced by the non-linearity of electronics below 5 MeV energy equivalent, which was fixed before 2017.

3 Clustering

All calorimeters of the CMD-3 detector have a common clustering approach. On the first step, the cores of the future clusters are searched. The cluster core is a channel with an energy greater than 5 MeV. After that all neighbouring channels with energies greater than 2 MeV are combined into the cluster. This process is repeated until the formed cluster has no neighbours above the low threshold. In the context of the strip system this procedure is independently performed for each side.

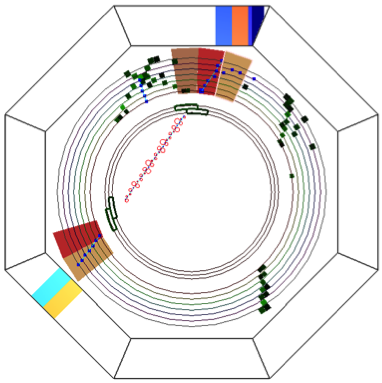

Figure 2: The CMD-3 event with cosmic ray.

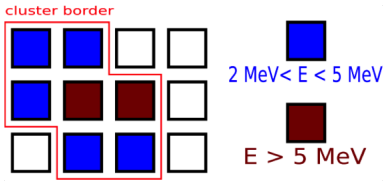

Figure 3: The scheme of the clustering approach.

The coordinate of the strip cluster is defined as the center of gravity by energy, thus the average spiral is formed. The average spirals on each side of the layer are intersected. After that the obtained points are approximated by a straight line as a particle track. The point on the closest layer to the detector axis is considered the conversion point of the EM-shower.

The formed clusters from each system should be merged into one full cluster. If there is at least one crystal of the CsI cluster within the angle range ($\delta_{\theta,\phi} = 0.2$) around the center of one tower from the LXe cluster, these clusters will be combined. The same procedure is performed for the LXe and BGO clusters. If the strip track goes within the LXe tower cluster, this is considered to belong to the same photon.

4 Separation of close photons

In addition to the high angular resolution of photons the strip structure of the LXe calorimeter provides a possibility to reconstruct close photons. This feature is especially important for multi-particle events and high energy neutral pions. For example, in the process $e^+ e^- \to \pi^0 \gamma$ the angle between photons from π^0 becomes comparable to the tower size at the π^0 exceeding 500 MeV. The standard clusterization procedure merges two photons if the opening angle between them is less than 0.4 radians.

We set the new parametrization of the strip system by the next formula:

$$\phi(R) \approx [\varphi_0 \pm tg(\theta)] + [r_{min} \pm Z_0] \cdot \frac{1}{R} + O(\frac{1}{R^2}),$$

where the photon trajectory is considered as a straight line with parameters: ϕ and θ — momentum angles, r_{min} and

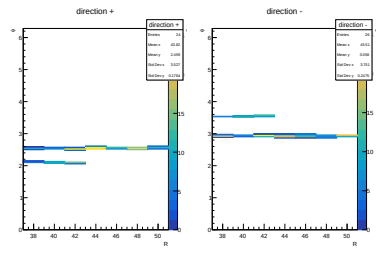

Figure 4: The example of the filtered strip tracks with the new parametrization in both strip directions.

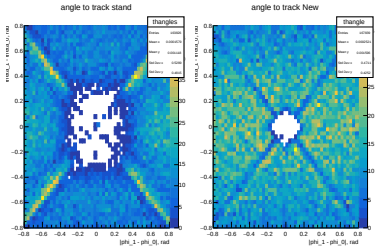

Figure 5: The comparison of the standard photon reconstruction (left) and the new approach (right) in case of two close photons. The difference between polar angles is on Y-axis and between azimuthal is on X-axis.

Z_0 — the closest point to the beam line, the sign ± (i.e. + or −) indicates the strip direction or side of the LXe layer. The parameters ϕ and R are the radial angle of the strip at start point of the spiral and radius of the strip layer, respectively. After that the single hits are filtered as shown in Fig. 4.

Then fits of obtained hit distribution assuming 1,2, ..., etc of horizontal lines (corresponding to the same number of particles) are performed. We minimize the following functional:

$$J_N = \sum_i A_i \cdot min(\phi_i - \phi_1(R_i); ...; \phi_i - \phi_N(R_i))^2,$$

where J_N is so-called moment of the N lines, A_i — amplitude of the strip, ϕ_i and R_i — angle and radius of the strip and $\phi_j(R)$ — angle of the line at R_i. The minimum operator connects the current hit with the closest line. The optimal number of lines is determined by the experimental classification parameter:

$$\sigma_N = \sqrt{J_N / \sum_i A_i} \propto R_M,$$

where σ_N characterizes the standard width of the EM-shower, which is approximately constant and proportional to Molière radius.

This approach drastically reduces the minimal angle between two separated photons as demonstrated by Fig. 5. As a result the efficiency of the high momentum π^0 reconstruction considerably increases as shown in Fig. 6.

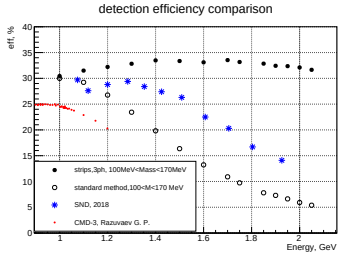

Figure 6: The efficiency distribution for the process $e^+ e^- \to \pi^0 \gamma$ for the CMD-3 and SND experiments. The CMD-3 results were obtained by three methods, the new approach gives the highest efficiency.

5 Photon energy reconstruction

Due to the energy leak as well as the energy loss in the inactive material in the calorimeter, the measured energy deposition does not equal to the initial photon energy. To reconstruct the photon energy we use the simulation as a reference. As described in the result of Sect. 2 the experiment data are in a good agreement with the EM-shower simulation. Initially, the energy range 0–1000 MeV is divided into 100 points. The photon EM-shower is simulated with a uniform angle distribution at each energy point. Assuming that the detector is uniform in the azimuthal angle the function $E_{dep} = f(E_\gamma, \theta)$ is obtained, where E_{dep} is a sum over the all calorimeters. This function is inverted numerically and interpolated in both directions, yielding $E_\gamma = f^{-1}(E_{dep}, \theta)$. The relative resolution of the photon energy in the simulation is $\sigma_E/E = \frac{0.036}{E[GeV]} \oplus 0.027$ in the barrel part and $\sigma_E/E = \frac{0.030}{E[GeV]} \oplus 0.019$ in the endcap range.

We also develop a new approach based on the neural networks. For now the preliminary results are obtained. First, the photons with the energy 700 to 800 MeV and only in the barrel parts are considered. The neural network has 5 inputs nodes: $E_{LXe}, E_{CsI}, \rho_{conv}, \theta_\gamma$ and ϕ_γ, where E_{LXe} and E_{CsI} — energy deposition in the system, ρ_{conv} — radius of the LXe layer where the conversion point occurs, θ_γ and ϕ_γ — reconstructed angles. The output node contains the true simulated photon energy. The neural network improves the resolution from 33.2 to 29.7 MeV in the simulation and from 38.2 to 33.1 MeV in the experimental data ($e^+ e^- \to \gamma\gamma$) for the photons with energies 700–800 MeV.

6 Conclusion

The combined LXe/CsI electromagnetic calorimeter is an important subsystem of the CMD-3 detector. This calorimeter provides a high precision measurement of the photon coordinates as well as high energy resolution for photons. However, the combined structure of the calorimeter requires sophisticated procedures of the photon reconstruction and energy calibration. This proceeding describes such procedures used in the CMD-3 experiments at present as well as the development of new instruments for photon reconstruction using the LXe strip system and the photon energy evaluation method based on the neural network approach.

References

[1] M.N. Achasov et al., The VEPP-2000 electron-positron collider: First experiments, JETP **113**, 213 (2011). 10.1134/S1063776111060136

[2] B.I. Khazin (CMD-3, SND), Detectors and physics at VEPP-2000, Nucl. Instrum. Meth. **A623**, 353 (2010).

[3] M.N. Achasov et al., First results of spherical neutral detector (SND) experiments at VEPP-2000, Prog. Part. Nucl. Phys. **67**, 594 (2012).

[4] A.V. Anisenkov et al., Status of the Liquid Xenon calorimeter of the CMD-3 detector, JINST **9**, C08024 (2014).

[5] V.M. Aulchenko et al., CsI calorimeter of the CMD-3 detector, JINST **10**, P10006 (2015).

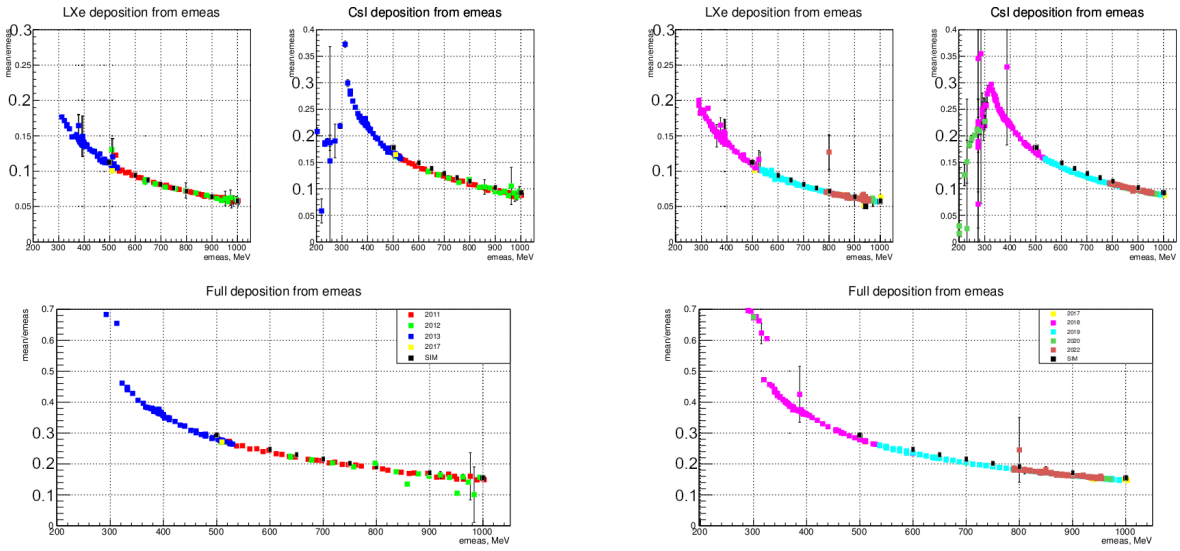

(a) The datasets before 2014.

(b) The datasets after 2014.

Figure 7: The dependency of the energy deposition in percent of the beam energy from the energy of the beam for the events with two MIPs. The top left figure is dedicated to the LXe-calorimeter, the right one to the CsI-calorimeter, and the bottom one to the combined. Different colors mean data sets in different seasons (or years).

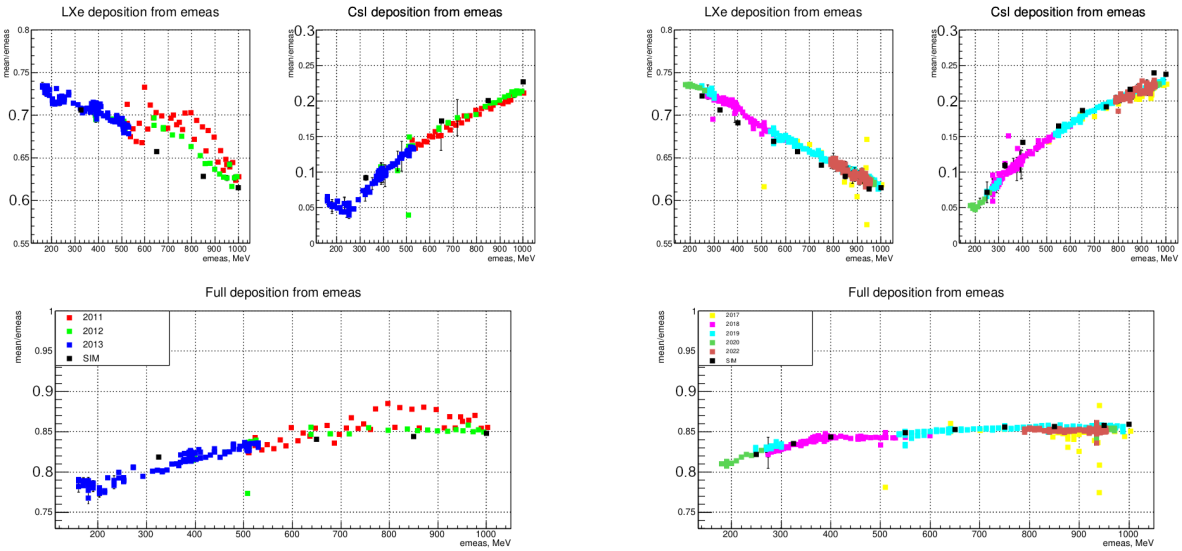

(a) The datasets before 2014.

(b) The datasets after 2014.

Figure 8: The dependency of the energy deposition in percent of the beam energy from the energy of the beam for the events with collinear electron and positron. The top left figure is dedicated to the LXe-calorimeter, the right one to the CsI-calorimeter, and the bottom one to the combined. Different colors mean data sets in different seasons (or years).